

Three-dimensional data of wirecut surface scans under the confocal microscope (110 character maximum, inc. spaces)

Yuhang Lin^{1,2,*}, Heike Hofmann^{2,3}, Curtis Mosher^{4,5}, Alicia L Carriquiry^{1,2}, Eden Amin², Jeff Salyards², and order? Jeff the last? check details? affiliations? Middle name for Alicia?¹

¹Iowa State University, Department of Statistics, Ames,

²Iowa State University, Center for Statistics and Applications in Forensic Evidence (CSAFE), Ames,

³University of Nebraska-Lincoln, Department of Statistics, Lincoln,

⁴Iowa State University, Department of Genetics, Development and Cell Biology (GDCB), Ames,

⁵Iowa State University, Roy J Carver High Resolution Microscopy Facility (HRMF), Ames,

*corresponding author(s): Yuhang Lin (yhlin@iastate.edu)

ABSTRACT

Update later: max of 170 words: describe the study, the assay(s) performed, resulting data, and reuse potential

Wire cut data is important in forensic investigations but lacks a systematic way of analyzing the data. We created a data set of 120 scans of aluminum wire cut in $\times 3p$ format, using 5 wire cutters and 3 locations along the 4 blades, with 2 replicates for each combination. A systematic pipeline with multiple analysis plots was developed to analyze the data and draw conclusions based on numerical measures.

Background & Summary

Wire cut data is a type of forensic tool mark data used to identify the source of a wire cutter based on the striations left on the surface. There have been cases where the evidence and testimony on wire cut evidence played a crucial role in the criminal investigation and conviction of a defendant.

However, there is a lack of a standardized method to analyze it except for visual comparison. Although the Association of Firearm and Toolmark Examiners (AFTE) developed the Theory of Identification¹, which outlines the process of comparing tool marks, it is still subjective and relies on the examiner's experience, making results hard to reproduce and validate. Several reports, such as those from the National Research Council² and the President's Council of Advisors on Science and Technology³, pointed out the abovementioned issues and called for more objective and reproducible methods to analyze tool marks. Early research by Ma et al.⁴ and Zheng et al.⁵ has focused on collecting and distributing datasets for this purpose and providing a foundation for future advancements in tool mark analysis. Studies such as those by Chu et al.⁶ and Vorburger et al.⁷ have demonstrated the efficacy of using numerical methods to improve accuracy and consistency in tool mark analysis. Hare et al.⁸ and Ju et al.⁹ have explored methods for quantifying the similarity between representative signals, but alignment remains a major hurdle.

In this study, we would like to follow the same path and provide a data set of wire cut scans, and also discuss a systematic pipeline to analyze the data and draw conclusions based on numerical measures. Here, we provide a data set containing multiple files, as described in Table 1.

For the reproducibility of all our data and alignment results, we introduce in detail in [Cutting wires](#) how we cut the wire and collect the 120 scans with 5 tools on 3 locations, in [Extract profiles](#) how we extract profiles from the scans, in [Filtered signals](#) how we filter signals from the profiles, in [Align signals](#) how we align signals from different scans and optimize the alignment with the cross-correlation function (CCF) values. In [Data Records](#), we discuss where our data is held. Then, in [Technical Validation](#), a technical validation was conducted to further compare signals from different sources also match our assumption, together with visual aids for drawing conclusions. Finally, in [Usage Notes](#), we provide available codes for creating the data set and conducting technical validation, as discussed in [Methods](#) and [Technical Validation](#). [Code availability](#) discusses where these codes can be found online. We hope this pipeline developed using this data set can be further generalized and applied to real crime scenes to help investigators draw conclusions based on real wire cut data.

Table 1. Structure of available data and files.

	Description	Section
Raw data		
scans /	folder containing 120 topographic 3d scans of aluminum wire cuts in x3p format	Cutting wires
meta.csv	meta information for each cut with tool, blade, and location information (csv format)	Cutting wires
Manual derivatives		
profiles	folder of files with manually extracted profiles (csv format)	Extract profiles
Computational derivatives		
signals	folder of signals, processed from corresponding profile (csv format)	Filtered signals
CCF values	CCF values of all pairwise aligned signals in 1 CSV	Align signals
Image files		
aligned-signals	pictures of pairwise aligned signals from same sources in PNGs	Align signals

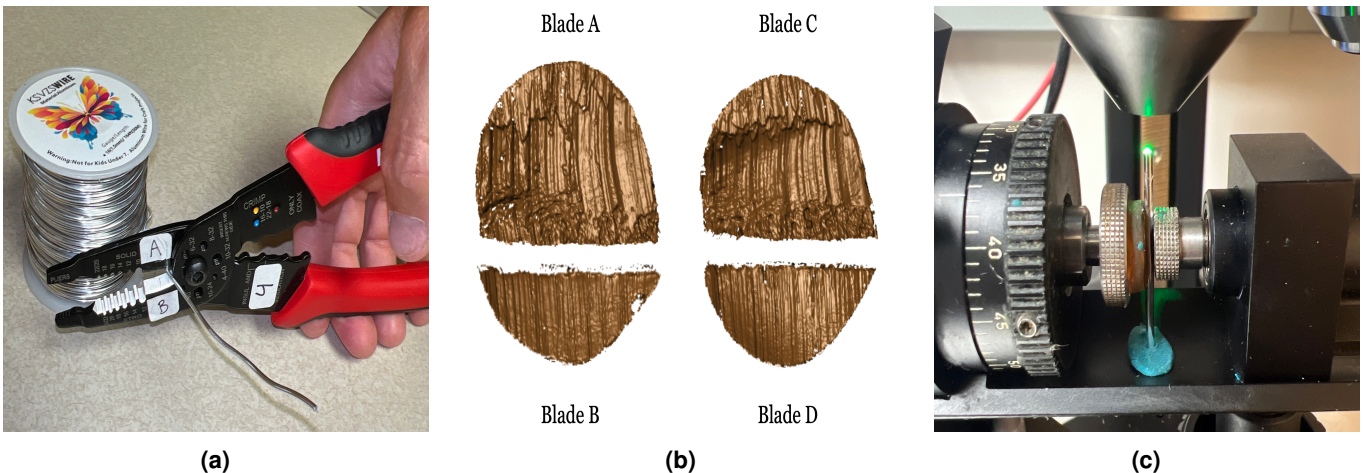


Figure 1. (a) A Kaiweets wire cutter of model KWS-105 was used to cut the wire. we don't have another high resolution pic showing wirecutter cutting wire (b) A tent structure created by blade AB. After separating 2 tent structures by the connecting position, we obtained 2 samples - 1 sample from blade A and B. (c) A confocal microscope was used to scan the wire surfaces. need an extra pic of the tip | full requirements see <https://www.nature.com/sdata/publish/submission-guidelines#figures>

42 Methods

43 In this study, aluminum wire was used to create an optimal scenario where the most amount of information could be transferred
 44 from the tool to the substrate, despite the wire in some real cases being made of lead. The physical property of aluminium
 45 wire make it an excellent candidate for keeping marks while being relatively easy to bend and non-toxic.

46 Cutting wires

47 The aluminum wire used was 16 Gauge/1.5 mm, anodized. In order to cut the wire, 4-inch pieces were unspooled and cut
 48 using Kaiweets wire cutters, model KWS-105, as shown in Figure 1a, for 1 blade location, either inner, middle, or outer,
 49 which gives us 1 replicate. Each piece was then cut into half to create 2-inch pieces for each side, AB and CD, with a sharpie
 50 line marking the cut ends, giving us 4 samples. Here, we are showing AB and CD sides in Figure 1b, with the back of A
 51 being C and the back of B being D. Both AB and CD sides form tent structures on the tips of the wire, and we can separate
 52 each side of the tent into 2 pieces along the bending position, resulting in 8 scans. We repeated this process for all 3 locations
 53 along the blade and 5 wire cutters, with 2 replicates for each tool-edge-location combination, resulting in 120 scans. Each
 54 piece was labeled with the naming conventions, T(ool) 1/2/3/4/5 (Edge) A/B/C/D W(ire) - L(ocation) I(nner)/M(idle)/O(uter)
 55 - R(epetition) 1/2, with T1AW-LI-R1 being the piece cut by tool 1 on the A edge at the inner location for the first repetition.
 56 Then, we can use the standard scanning protocols for the confocal microscope, shown in Figure Figure 1c, to scan the wire tip
 57 surfaces. The scanned surfaces are saved in a resolution of $0.645\mu\text{m} \times 0.645\mu\text{m}$ per square pixel in an x3p file format.

58 Extract profiles

59 Numerical comparisons between 2 replicates cannot be done directly on the x3p files. We need to extract representative
 60 functions from the scans first. A representative function with the most information is considered as a signal for one scan,
 61 which can be used for comparison later. To obtain this function, we first need a profile of the scan, which is a sequence of
 62 values along a user-drawn line on the surface. The profile should capture most features of the scan, and be orthogonal to the
 63 striation marks of the scan, which are formed by ups and downs of grooves. So, we draw the line across the wide region of
 64 the scan to maximize the feature captured, as shown in dark blue in Figure 2(a). We can then investigate the values under this
 65 profile line. The profile function is along the line is plotted in Figure 2(b).

66 Filtered signals

67 With the profile extracted, we can then obtain the signal. Two Gaussian filters are applied to these resulting profiles. In
 68 particular, we first used a large low-pass filter with bandwidths of 400 microns to remove large trend, as it can overwhelm the
 69 signals, and then used a small high-pass filter of 40 microns to average across noise and remove spikes, as shown in Figure
 70 2(c). Cleveland et al.¹⁰ (add reference: W. S. Cleveland, E. Grosse and W. M. Shyu (1992) Local regression models. Chapter

71 8 of Statistical Models in S eds J.M. Chambers and T.J. Hastie, Wadsworth & Brooks/Cole.). Finally, the extreme tail values
72 are removed.

73 Align signals

74 Signals extracted from different scans can be put together for comparison, and we maximize the cross-correlation function
75 (CCF) values between the signals to numerically find the best alignment. For example, we compare T1AW-LI-R1 to T1AW-
76 LI-R2, T1CW-LI-R1 to T1CW-LI-R2, and so on. That is comparing each row in Figure 3. We know that signals from two
77 replicates with the same tool-edge-location combination should yield similar signals as in the first and second column of
78 Figure 4, which will give alignments of massive overlapping and high CCF values close to 1. The alignments and values we
79 got in the rightmost column of Figure 4 fulfill our expectations.

80 Data Records

81 The complete data set is available on the ISU DataShare repository at <https://iastate.figshare.com/>, which is public and open
82 access for every interested researcher. The data set consists of 120 scans in the x3p file format with the naming convention
83 as described before. (Explain the x3p header info?)

84 Technical Validation

85 a picture of alignment with ccf from different sources to show if different source, our evaluation returns small ccf, which
86 matches what we thought.

87 For the data collection process, two team members did the cutting and labeling together, then one person did the scanning
88 and named according to the naming convention above. The scanning was done in a specific order to ensure consistency across
89 all scans. The data was saved in a consistent format to ensure they could be easily accessed and analyzed. A third person then
90 checked the data to ensure that the data was consistent in naming and accurate.

91 For the validation of the scans and their processing we investigate the correlation scores of pair-wise aligned signals. For
92 signals from scans of wires cut with a different tool, we would expect a low correlation score. Large scores between signals
93 are indicative of being made by the same tool. Show boxplots and roc curve.

94 For the validation of all other tools and locations of scan replicates, see [Github repo](#).

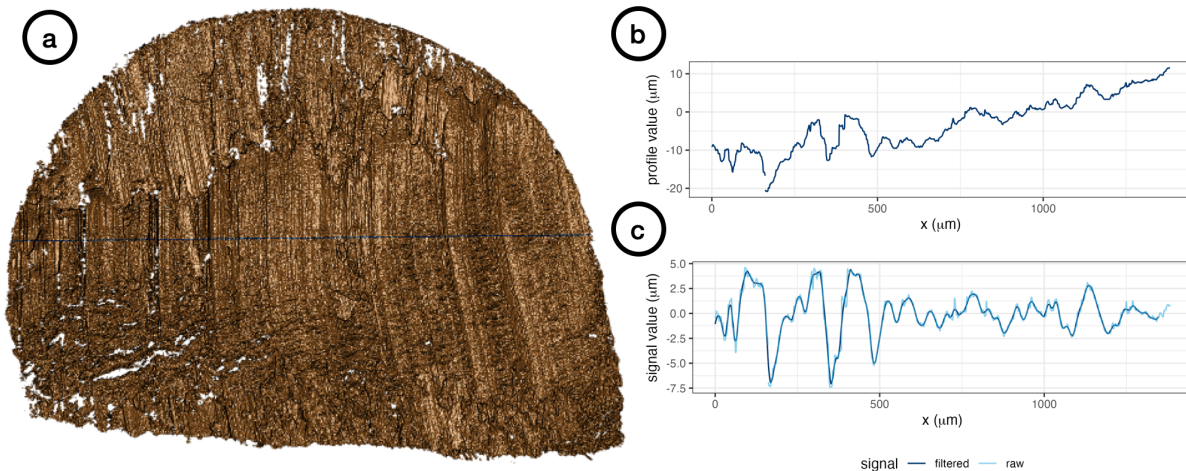


Figure 2. (a) A profile line in dark blue was drawn across the striations of the scan. (b) The profile function extracted along the profile line in (a). (c) The raw signal in light blue is obtained by using the low-pass filter on the profile function in (b) and the filtered signal is obtained by using the high-pass filter on the raw signal.

95 Usage Notes

96 The R package `x3ptools` (available from CRAN) supports working with files in x3p format.

97 Sample scripts in R for processing scans from x3p format to their signal are available from ... [github](#).

98 Further analysis can be conducted with the GitHub R package `wire` and the GitHub R shiny app `wireShiny` ([citation?](#)). We already conduct between-replicate comparisons in the technical validation section, and we can also conduct
99 across-replicate comparisons to establish error rates threshold and produce other analysis plots.
100

101 Suppose we put the CCF values in a tilemap with different tool, location and edge combinations. In that case, we expect
102 only the diagonal to have high CCF values, close to 1 and marked as orange in the tilemap, as the diagonal represents the same
103 source, and the rest of the matrix to have low CCF values, close to 0 and marked as gray. In Figure 5, the behavior is consistent
104 with our expectation overall, except for some rare cases with tool 5 edge D, which is caused by [?????](#). We also put the resulting
105 CCFs in the boxplot, as in Figure 6. We can see that the CCF values for the same sources are close to 1, while the CCF values
106 for different sources are much lower than expected. This difference can be used to establish a threshold for CCF and help us
107 draw conclusions about the similarity between wire cut scans numerically, which can be used in real crime scenes. The density
108 plot in Figure 7 shows the distribution of the CCF values with the same sources and different sources. The overlapping points
109 between the tails of these two distributions can be a rough threshold. Furthermore, the receiver operating characteristic (ROC)
110 curve in Figure 8 shows the sensitivity / true positive rate against the false positive rate (FPR) (1 - specificity). The curve is
111 very close to the upper left corner, which is excellent for classification and drawing conclusion. It gives us a true threshold of
112 0.589 to control the FPR to be less than 0.05 with false negative rate (FNR) to be 0, ([false positive rate \(FPR\) / false discovery](#)
113 [rate \(FDR\) -> define the H0 or call it false identification rate \(FIR\)???](#)), and 0.658 to control the FPR to be less than 0.01, with
114 FNR to be 0.02.

115 **Code availability**

116 [table of code](#)list files with short explanation, similar to table 1

117 no, we can't use the website as a place for more detailed procedures. This paper is the detailed procedure.[no more](#)
118 [README, scanning procedures in another HTML](#)

119 We put together the cutting and the standard scanning procedures mentioned in Section [cross-ref not working](#) with more
120 pictures for each step into a [README of the GitHub repository heike/Wirecuts](#) ([High-res pics needed in the README](#)).

121 The data set can be easily accessed with the CRAN R package `x3ptools`. Further analysis can be conducted with the
122 GitHub R package `wire` and the GitHub R shiny app `wireShiny` ([citation](#)).

123 **References**

- 124 1. AFTE. The association of firearm and tool mark examiners: Theory of identification as it relates to toolmarks. *AFTE J.*
125 **30**, 86–88 (1998).
- 126 2. NRC. *National Research Council: Strengthening Forensic Science in the United States: A Path Forward* (National
127 Academies Press, 2009).
- 128 3. President's Council of Advisors on Science and Technology. *President's Council of Advisors on Science and Technology: Forensic Science in Criminal Courts: Ensuring Scientific Validity of Feature-Comparison Methods* (Executive Office of
129 the President of the United States, President's Council, Washington, D.C., 2016).
- 130 4. Ma, L. *et al.* NIST Bullet Signature Measurement System for RM (Reference Material) 8240 Standard Bullets. *J. Forensic
131 Sci.* **49**, 1–11, [10.1520/JFS2003384](https://doi.org/10.1520/JFS2003384) (2004).
- 132 5. Zheng, X. A., Soons, J. A. & Thompson, R. M. NIST Ballistics Toolmark Research Database | NIST (2016).
- 133 6. Chu, W., Thompson, R. M., Song, J. & Vorburger, T. V. Automatic identification of bullet signatures based on consecutive
134 matching striae (CMS) criteria. *Forensic Sci. Int.* **231**, 137–141, [10/gn65cz](https://doi.org/10/gn65cz) (2013).
- 135 7. Vorburger, T. *et al.* Applications of cross-correlation functions. *Wear* **271**, 529–533, [10.1016/j.wear.2010.03.030](https://doi.org/10.1016/j.wear.2010.03.030) (2011).
- 136 8. Hare, E., Hofmann, H., Carriquiry, A. *et al.* Automatic matching of bullet land impressions. *The Annals Appl. Stat.* **11**,
137 2332–2356, [10.1214/17-AOAS1080](https://doi.org/10.1214/17-AOAS1080) (2017).
- 138 9. Ju, W. & Hofmann, H. The R Journal: An Open-Source Implementation of the CMPS Algorithm for Assessing Similarity
139 of Bullets. *The R J.* **14**, 267–285, [10.32614/RJ-2022-035](https://doi.org/10.32614/RJ-2022-035) (2022).
- 140 10. Cleveland, W. S., Grosse, E. & Shyu, W. M. Local Regression Models. In *Statistical Models in S* (Routledge, 1992).

142 **Acknowledgements**

143 This work was partially funded by the Center for Statistics and Applications in Forensic Evidence (CSAFE) through Cooper-
144 ative Agreement 70NANB20H019 between NIST and Iowa State University, which includes activities carried out at Carnegie
145 Mellon University, Duke University, University of California Irvine, University of Virginia, West Virginia University, Univer-
146 sity of Pennsylvania, Swarthmore College and the University of Nebraska-Lincoln.

147 **Author contributions statement**

148 Let's follow the Elsevier definitions: <https://www.elsevier.com/researcher/author/policies-and-guidelines/credit-author-statement>

149 Y.L.: Methodology, Software, Validation, Data Curation, Writing - Draft; H.H.: Conceptualization, Methodology, Valida-
150 tion, Writing - Review & Editing; C.M.: Lab supervision; E.A.: Physical Specimen, Scanning; J.S: Forensic advice; A.C.:
151 Funding acquisition.

152 All authors reviewed the manuscript.

153 **Competing interests**

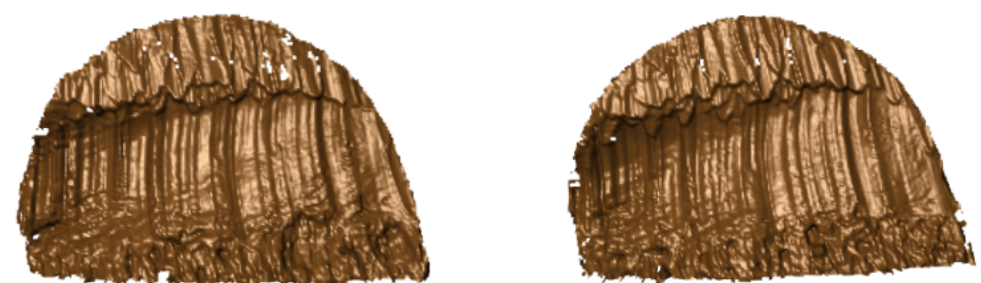
154 (mandatory statement)

155 H.H. is a technical advisor to AFTE (Association of Firearms and Toolmarks Examiners), fellow of the ASA (American
156 Statistical Association), and committee member of the ASA Forensic Science Committee. H.H. has testified as court witness
157 on behalf of judge April Neubauer, NY State Supreme Court Criminal Term in New York City. [other competing interests -](#)
158 [Alicia?](#)

Edge A



Edge C



Edge B



Edge D

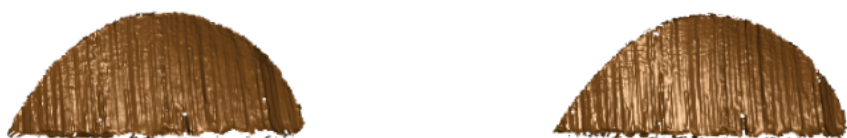


Figure 3. Scans from different sides of tool 1 at the inner location.

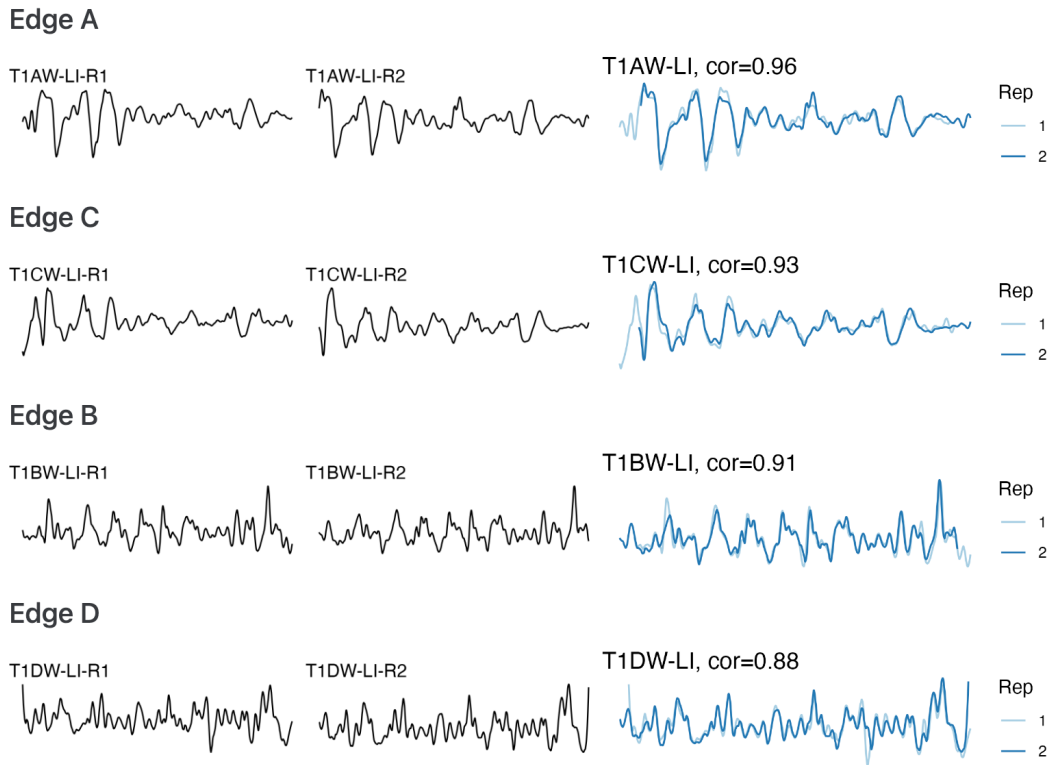


Figure 4. The first and second columns show the signals extracted from Figure 3, and the third column shows the alignments and CCF values between pairs of signals.

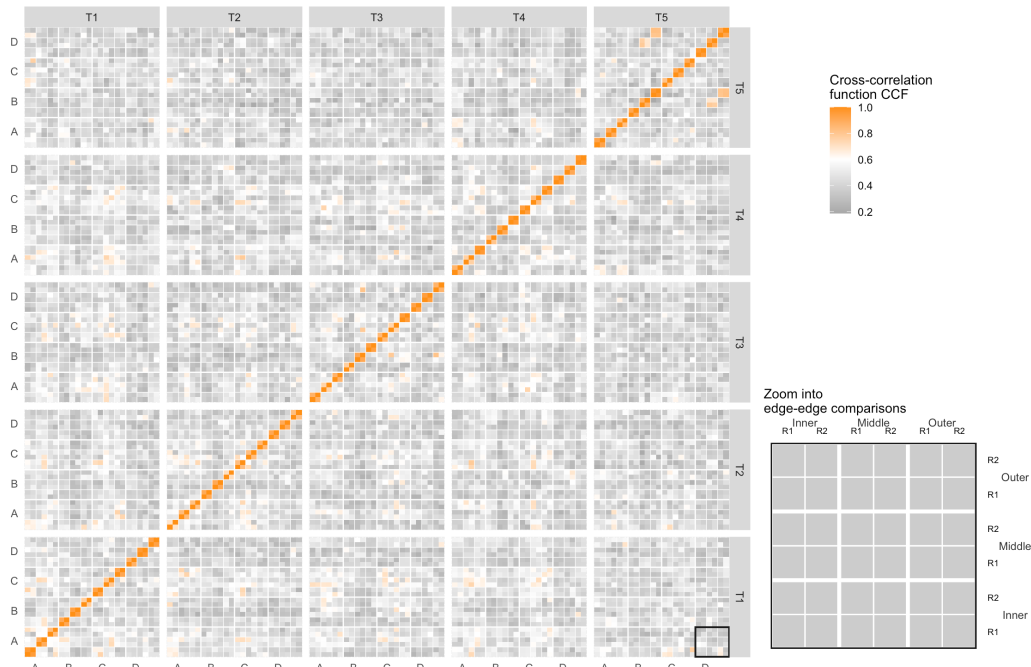


Figure 5. The tilemap shows signals from the same source have CCFs close to 1.

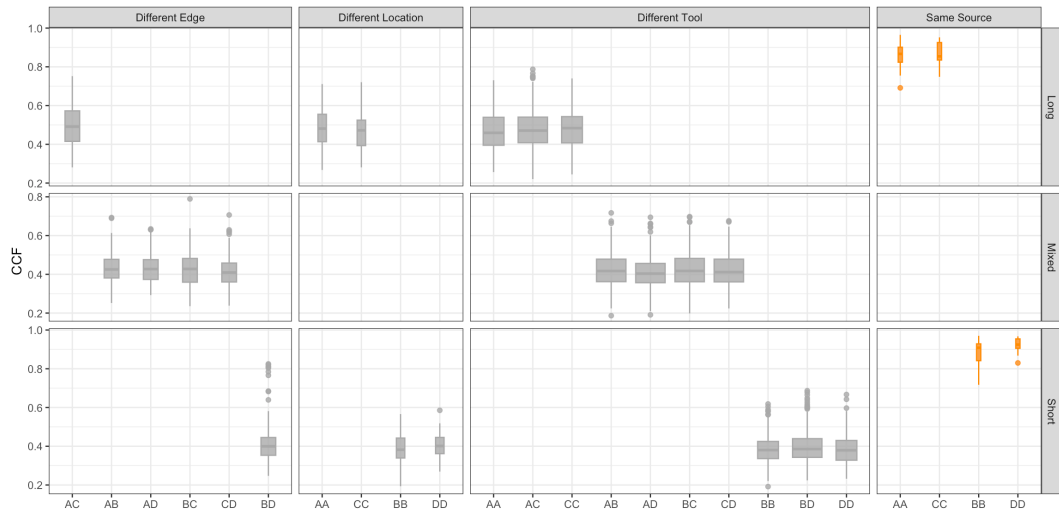


Figure 6. The boxplot shows that signals from the same sources have higher CCFs than those from different sources.

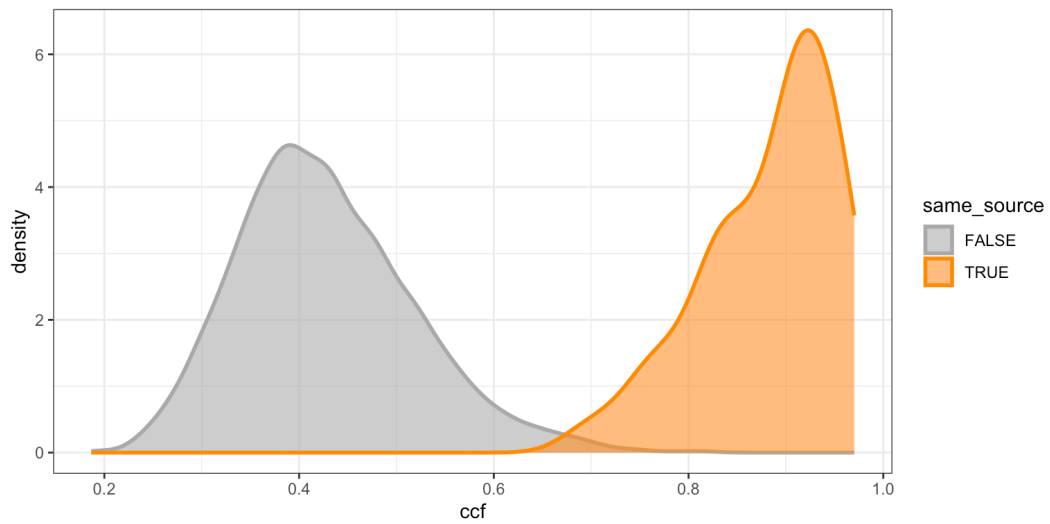


Figure 7. The density plot shows tails of distributions overlap, which can be used as a rough threshold for drawing conclusions.

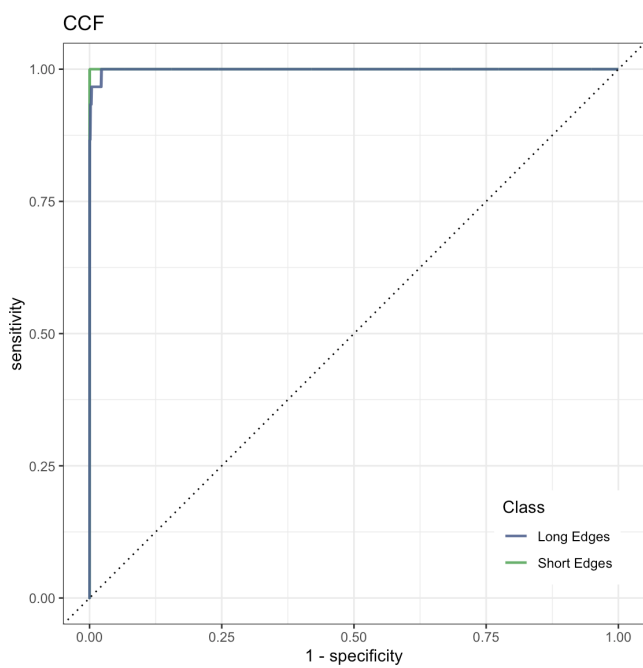


Figure 8. The ROC curve is bending very close to the upper left corner, which means excellent in classification and drawing conclusions.